applied sciences

MDPI

Article

Granular Media Friction Pad for Robot Shoes—Hexagon Patterning Enhances Friction on Wet Surfaces

Halvor T. Tramsen, Lars Heepe and Stanislav N. Gorb *

Department of Functional Morphology and Biomechanics, Zoological Institute, Kiel University, 24118 Kiel, Germany; htramsen@zoologie.uni-kiel.de (H.T.T.); lheepe@zoologie.uni-kiel.de (L.H.)
* Correspondence: sgorb@zoologie.uni-kiel.de

Abstract: For maximizing friction forces of robotic legs on an unknown/unpredictable substrate, we introduced the granular media friction pad, consisting of a thin elastic membrane encasing loosely filled granular material. On coming into contact with a substrate, the fluid-like granular material flows around the substrate asperities and achieves large contact areas with the substrate. Upon applying load, the granular material undergoes the jamming transition, rigidifies and becomes solid-like. High friction forces are generated by mechanical interlocking on rough substrates, internal friction of the granular media and by the enhanced contact area caused by the deformation of the membrane. This system can adapt to a large variety of dry substrate topologies. To further increase its performance on moist or wet substrates, we adapted the granular media friction pad by structuring the outside of the membrane with a 3D hexagonal pattern. This results in a significant increase in friction under lubricated conditions, thus greatly increasing the universal applicability of the granular media friction pad for a multitude of environments.

Keywords: friction; lubrication; jamming; granular media; structured silicone membrane; hexagon pattern; biomimetics; bioinspired surfaces; anti-slip systems; contact mechanics; recycling; robotics

Citation: Tramsen, H.T.; Heepe, L.; Gorb, S.N. Granular Media Friction Pad for Robot Shoes—Hexagon Patterning Enhances Friction on Wet Surfaces. *Appl. Sci.* **2021**, *11*, 11287. https://doi.org/10.3390/app112311287

Academic Editor: Nuno Miguel Fonseca Ferreira

Received: 11 October 2021
Accepted: 24 November 2021
Published: 29 November 2021

1. Introduction

Generating large friction forces on unknown substrate geometries requires high adaptability when approaching the substrate, combined with high energy dissipation when applying transversal load. This is why we recently proposed the granular media friction pad (GMFP) as a potential universal solution for friction enhancement on a wide range of substrates [1].

The GMFP consists of a thin elastic membrane encasing granular material, such as sand, metal powder, plant seeds, etc. When applying load to the GMFP, the granular medium undergoes the jamming transition [2,3]. The result of this is fluid-like behavior [4,5] of the GMFP, when unloaded or approaching the substrate topography (see Figure 1a), and solid-like behavior, when pressed against the substrate (see Figure 1b). Friction forces are generated by the mechanical interlocking of the now solid-like granular material and the substrate asperities, as well as by high internal friction of the granular media [6–11]. When taking away the normal load and pushing the GMFP onto the substrate, the granular filling becomes fluid-like again, enabling easy removal from the substrate without requiring high pull-off forces. In addition to this, the thin elastic encasing membrane holding the loosely filled granular material can create large contact areas with the substrate, contributing to the total resulting friction force by adhesion-mediated friction [12–14] and by elastic deformation of the soft membrane. In contrast to previous systems employing the jamming transition to create friction or holding forces [4,15–20], no active control mechanism (such as the application of a vacuum to control the jamming transition) is needed.

While the GMFP can adapt to a large variety of substrate topologies and form around contaminating particles embracing them [21], this type of structure would probably fail on

wet substrates due to its extremely smooth membrane [22–24] and the resulting hydrodynamic lubrication when sliding over a substrate.

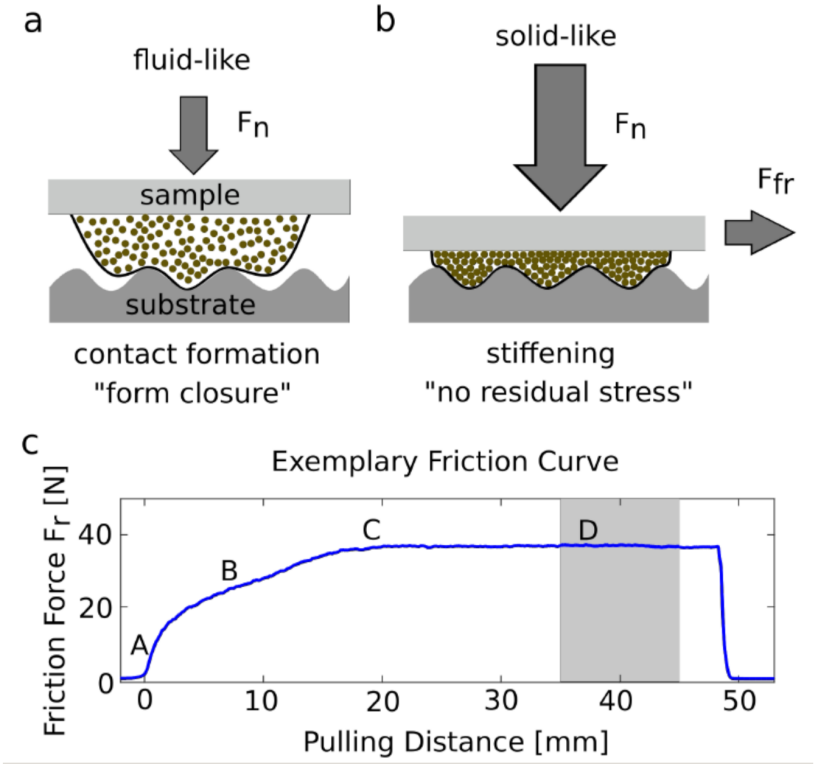

Figure 1. Granular media friction pad (GMFP). (**a**) Fluid-like behavior when coming into contact with a substrate [1], (**b**) solid-like behavior upon applying normal load (jamming transition), (**c**) exemplary friction curve showing the four phases of a pulling curve at a normal load F_n = 19.36 N: (A) initial shearing of jammed granular media, (B) stretching of the membrane in addition to granular media shearing, (C) maximum static friction force and onset of global dynamic friction, (D) dynamic sliding of the entire membrane.

In nature, numerous animals live in moist or wet environments, but are still able to get a stable grip for secure attachment and locomotion [25]. For a large variety of these animals, a convergent solution appeared in the course of biological evolution to achieve this: microstructuring their attachment pad surface [26,27] with mostly hexagonal arrays of channels, as seen, e.g., in a large diversity of frogs [25,26,28], in bush crickets [27,29], stick and leaf insects [30], and salamanders [31,32]. The microstructure not only helps in spreading secretory fluid over the whole attachment pad for adhesion enhancement, but also to remove surplus fluids and enable intimate contact with the substrate [25,33,34] when gripping but also while sliding. This principle has been adapted in several biomimetic studies both for similar dimensions [22,26,27,32,35] as well as for much larger structures, such as those in the tire industry [27,36–38].

While microstructuring of a surface is highly effective for draining fluids and to enable high friction forces on smooth substrates, a second principle can be observed in nature in conforming to wet (or rough) substrates to enhance contact area for friction [39]: The microstructured attachment pads feature a complex superstructure inside, which results in extremely soft attachment pads. This can be done actively [40–42] or passively by design [25,29,33,39,43,44].

In this study, we combine the structuring of the membrane with extreme softness and adaptability by enhancing the membrane surface with a hexagon pattern. An increase in friction on wet substrates is expected, while maintaining fluid-like behavior when approaching a rough or contaminated substrate to maximize the contact area. We investigate

the friction performance of smooth and hexagonally patterned GMFP on a flat substrate when dry, and also when completely immersed in mineral oil.

2. Materials and Methods

The granular media friction pad (GMFP) was composed of loose granular material that was encased by a thin, elastic membrane. The membrane was put flat on a lightweight, 3D-printed sample holder and clamped down using an adjusting washer (40 mm × 50 mm × 1 mm). Then, the granular material (1.7 ground coffee, Gold 100% Arabica, Markus Kaffee GmbH & Co., KG, Weyhe, Germany, see [1] for more details) was pushed behind the membrane through the lockable hole of the sample holder.

Two different types of GMFP were investigated: one with a smooth membrane (see Figure 2a), and one with a hexagon-patterned membrane (see Figure 2b). The membranes, consisting of Dragon Skin^{TM} 30 (Smooth-On, Inc., Macungie, PA 18062, USA) with a Young's Modulus of 0.53 ± 0.02 MPa, were cast by pouring the uncured resin between two plastic foils, which were fixated on glass plates and separated by 1 mm spacers. This resulted in a 1 mm thick silicone membrane. For the hexagon membrane, a hexagon grid with 2.19 mm circumcircle, 0.4 mm groove width and 0.6 mm groove depth was 3D-printed from PLA using an Original Prusa i3 Mk3 (Prusa Research s.r.o., Prague, Czech Republic). The grid was glued onto one of the plastic foils, before molding the membrane in the same way as the smooth membrane, so that the tops of the resulting hexagonal pillars had the same surface properties as the smooth membrane. There are three reasons for the selection of the hexagonal pattern: (1) As mentioned above, many biological systems use this evolutionarily optimized pattern for the purpose of grip enhancement on wet substrates [22,25,26,36–39]. (2) This pattern has been previously shown to enhance friction on substrates wetted by water [23,27,36–38]. (3) This pattern is relatively easy to design and adapt to curved substrates.

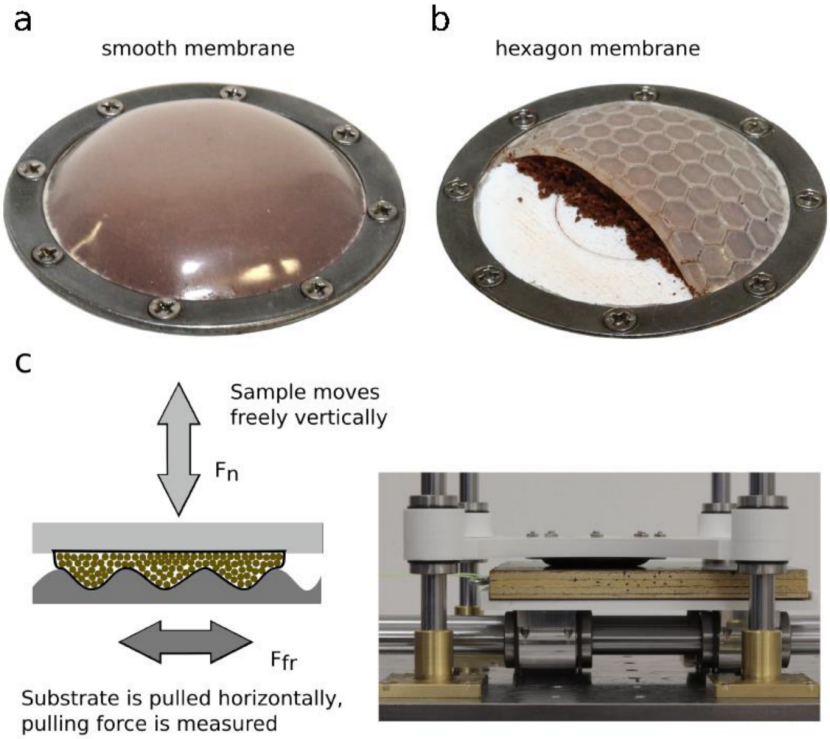

Figure 2. GMFP and experimental setup. (**a**) Photograph of a GMFP with a smooth membrane, (**b**) photograph of a GMFP with a hexagonally patterned membrane; the membrane is cut open, showing the GMFP's ground coffee filling, (**c**) schematic representation (left) and photograph (right) of the experimental setup.

The GMFP fixed to the sample holder could slide freely on four vertical linear rods using low-friction linear bearings (see Figure 2c). The substrate, the flat side of wire mesh plywood (100 mm × 100 mm), was pulled horizontally below the GMFP at 1 mm/s for 50 mm using a linear testing machine (Xforce HP 500 N, ZwickiLine, Zwick Roell, Ulm, Germany) that measured the pulling force. To obtain the sliding friction force, the pulling force was averaged for 10 s, 35 s after sliding started (see grey area in Figure 1c). To increase the normal load, F_n, additional weights could be placed on top of the GMFP. The coefficient of friction, μ, was obtained as $\mu = F_{fr}/F_n$.

To examine the effect of membrane structuring on the friction performance of the GMFP under dry and lubricated conditions, both the smooth and the hexagon-patterned GMFP were produced 12 times and tested subsequently on a dry substrate and on an oily substrate. For the latter, mineral oil (Mineral oil 330779, Sigma-Aldrich Chemie GmbH, Taufkirchen, Germany) was poured onto the substrate with a depth of at least 3 mm to fully submerge the contact area between the GMFP and substrate. For each sample and substrate combination, friction measurements were conducted at four different normal loads ranging from the sample weight itself (1 N) up to a maximum normal load of 19.36 N.

3. Results

The friction performance of the GMFP with smooth and hexagon-structured membranes on a dry substrate and submerged in mineral oil is illustrated in boxplots showing the average pulling force (see Figure 3a) and the resulting friction coefficient, μ (see Figure 3b). The average friction coefficients of all sample and substrate combinations for the four applied normal loads are shown in Table 1. For all normal loads, the different GMFP membranes, as well as the contamination of the substrate, led to a significant difference in the friction coefficients (Kruskal–Wallis rank sum test, Holm FWER method).

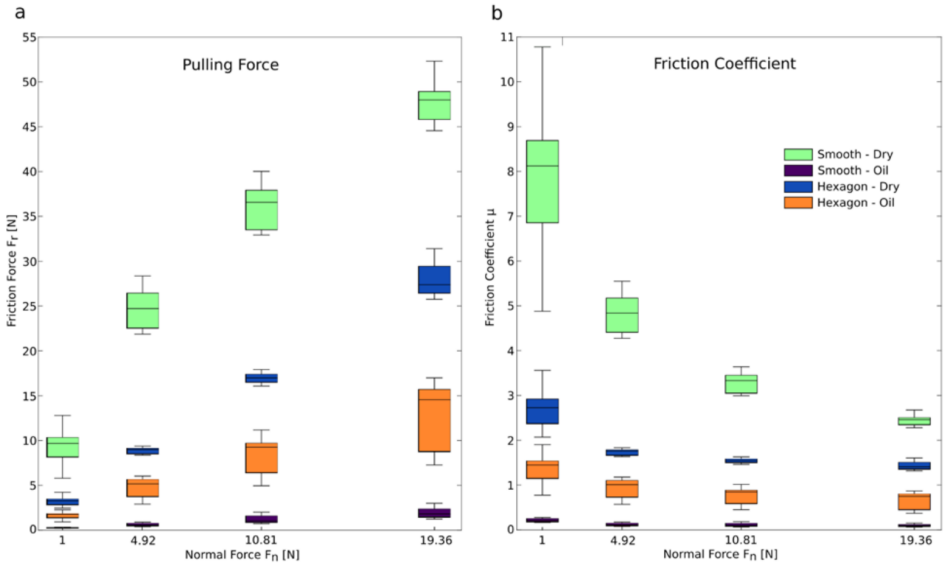

Figure 3. Friction performance of the smooth and hexagon GMFP on dry and oily substrate. (**a**) Measured friction force, (**b**) resulting friction coefficient. The boxes display the median and 25 and 75 percentiles with the whiskers indicating the most extreme data points.

Table 1. Average friction coefficients with standard deviation of the smooth and hexagon GMFP on dry substrate and when completely submerged under mineral oil for all normal loads.

Fn [N]	Smooth		Hexagon	
	Dry	Oil	Dry	Oil
1.00	7.9 ± 1.5	0.2 ± 0.1	2.7 ± 0.4	1.4 ± 0.3
4.92	4.8 ± 0.4	0.1 ± 0.1	1.7 ± 0.1	0.9 ± 0.2
10.81	3.3 ± 0.2	0.1 ± 0.1	1.5 ± 0.1	0.8 ± 0.2
19.36	2.5 ± 0.1	0.1 ± 0.1	1.4 ± 0.1	0.7 ± 0.2

3.1. Dry Substrate

On the dry substrate, the GMFP with a smooth membrane performs much better than the hexagon-patterned sample. The smooth GMFP achieves extremely high friction forces at a low normal load, with the highest friction coefficient being $\mu = 7.9 \pm 1.5$ at the lowest normal load of 1 N. At the highest normal load of 19.36 N, the sample (4 cm diameter) achieves friction forces up to 52 N.

Hexagonal structuring leads to a significant reduction in friction forces on the dry substrate. The friction coefficient is still between $\mu = 1.4$ and $\mu = 2.7$ for all loading conditions examined, but generated friction forces are only about half of those of the smooth membrane.

3.2. Oiled Substrate

While the smooth GMFP performs better on the dry substrate than the hexagon GMFP, the opposite is the case once it is submerged in mineral oil. Here, the smooth GMFP is only able to create a maximum of 3 N friction force under any loading condition, with the friction coefficient, μ, ranging from 0.1 to 0.2. In contrast, the hexagonal-patterned GMFP still achieves high friction forces with a friction coefficient (μ) of 0.7–1.4.

4. Discussion

On the dry substrate, the better friction performance of the smooth GMFP results from the larger contact area [12,13,45] in contrast to the grooved pattern of the hexagon membrane. It is known that soft, smooth rubber on a smooth glass surface can reach a frictional coefficient of $\mu = 2.8$ [46]. The observed experimental result, where the coefficient of friction decreases with an increasing normal load (Figure 3b), can be explained by the relatively stronger contribution of adhesion at lower loads. This is not surprising for relatively smooth and soft contact pairs and was previously observed in [47].

In addition, the deformation of the hexagon pillars during sliding could reduce the occurring friction forces by decreasing contact area even further [22,47–49]. However, for structured and microstructured surfaces, a reduction in uncontrolled stick-slip friction is expected due to a distribution of the crack propagation to the individual hexagonal pillars, which could result in higher peeling forces [27].

Submerged in oil, the picture is inverted: The lubrication never breaks down for the smooth membrane, resulting in extremely low friction coefficients. For the hexagon GMFP, however, breakdowns of the lubrication film and high friction forces occur. The drainage channels between the hexagonal pillars have to be large enough for draining the lubricant, depending on the viscosity of the lubricating fluid [25,27], the cross-section of the channels [25,27], and the sliding velocity [32,41], while still maintaining a pillar size sufficient for large contact areas. In the case of the GMFP, the deformation of the thin elastic membrane under normal load and also from stretching during sliding results in different channel geometries (depending on substrate, loading condition and occurring friction forces). The bending of the hexagonal pillars [22,48,49], which reduces the contact area during sliding, has to be considered as well. The effect of the friction enhancement of micropatterned surfaces in oil is potentially even stronger in water [27], because oil

has much higher wetting properties on all the surfaces and has much higher viscosity than water.

In this study, the number of sliding cycles was relatively low. After running in, the coefficient of friction might change due to the changes of the surface structure through abrasive wear. Our experimental design was selected to avoid the influence of wear on the results of our tests. In the future, tests with a high number of cycles would be desirable to study frictional behavior of both types of surface structure after running in (in the presence of wear).

For a further optimization of friction forces, the sliding direction of the hexagon GMFP could be considered. In our experiment, all hexagonal GMFPs were tested in the same orientation, i.e., with the side of the hexagons facing the sliding direction. In [26], an increase of up to 20% in friction force was observed when sliding with the hexagon tips forward. Even higher geometry-dependent anisotropies were observed for elongated pillar shapes due to drainage flow and a change in tangential contact stiffness [27,35]. This effect could be especially beneficial for an adapted hexagonal GMFP, when the sliding direction is predictable, or when friction anisotropy is desired.

Author Contributions: Conceptualization, L.H. and S.N.G.; methodology, L.H. and S.N.G.; software, H.T.T.; validation, H.T.T. and L.H.; formal analysis, H.T.T.; investigation, S.N.G.; resources, H.T.T.; data curation, H.T.T.; writing—original draft preparation, H.T.T.; writing—review and editing, L.H. and S.N.G.; supervision, S.N.G.; project administration, L.H. and S.N.G.; funding acquisition, S.N.G. All authors have read and agreed to the published version of the manuscript.

Funding: This research received no external funding.

Data Availability Statement: Data available on request from the authors.

Acknowledgments: We thank Hamed Rajabi for discussions and helpful comments. This work was partially supported by the German Science Foundation (DFG GO 995/34-1) within the framework of the special priority program "Soft Material Robotic Systems" (SPP2100 SMRS) to SNG.

Conflicts of Interest: The authors declare no conflict of interest.

References

1. Tramsen, H.; Filippov, A.E.; Gorb, S.N.; Heepe, L. Maximizing Friction by Passive Jamming. *Adv. Mater. Interfaces* **2020**, *7*, 1901930. [CrossRef]
2. Jaeger, H.M. Celebrating soft matter's 10th anniversary: Toward jamming by design. *Soft Matter* **2015**, *11*, 12–27. [CrossRef]
3. Majmudar, T.S.; Sperl, M.; Luding, S.; Behringer, R.P. Jamming transition in granular systems. *Phys. Rev. Lett.* **2007**, *98*, 058001. [CrossRef]
4. Brown, E.; Rodenberg, N.; Amend, J.; Mozeika, A.; Steltz, E.; Zakin, M.R.; Lipson, H.; Jaeger, H.M. Universal robotic gripper based on the jamming of granular material. *Proc. Natl. Acad. Sci. USA* **2010**, *107*, 18809–18814. [CrossRef]
5. Jaeger, H.M.; Nagel, S.R.; Behringer, R.P. Granular solids, liquids, and gases. *Rev. Mod. Phys.* **1996**, *68*, 1259–1273. [CrossRef]
6. Miller, B.; O'Hern, C.; Behringer, R.P. Stress fluctuations for continuously sheared granular materials. *Phys. Rev. Lett.* **1996**, *77*, 3110. [CrossRef] [PubMed]
7. Albert, I.; Sample, J.G.; Morss, A.J.; Rajagopalan, S.; Barabási, A.L.; Schiffer, P. Granular drag on a discrete object: Shape effects on jamming. *Phys. Rev. E* **2001**, *64*, 61303. [CrossRef] [PubMed]
8. Forterre, Y.; Pouliquen, O. Flows of dense granular media. *Annu. Rev. Fluid Mech.* **2008**, *40*, 1–24. [CrossRef]
9. Bi, D.; Zhang, J.; Chakraborty, B.; Behringer, R.P. Jamming by shear. *Nature* **2011**, *480*, 355–358. [CrossRef]
10. Corwin, E.I.; Jaeger, H.M.; Nagel, S.R. Structural signature of jamming in granular media. *Nature* **2005**, *435*, 1075–1078. [CrossRef]
11. Cates, M.E.; Wittmer, J.P.; Bouchaud, J.P.; Claudin, P. Jamming, force chains, and fragile matter. *Phys. Rev. Lett.* **1998**, *81*, 1841–1844. [CrossRef]
12. Persson, B.N.J. Silicone rubber adhesion and sliding friction. *Tribol. Lett.* **2016**, *62*, 1–5. [CrossRef]
13. Popov, V.L. *Contact Mechanics and Friction*; Springer: Berlin/Heidelberg, Germany, 2010.
14. Persson, B.N.J. Theory of rubber friction and contact mechanics. *J. Chem. Phys.* **2001**, *115*, 3840–3861. [CrossRef]
15. Amend, J.R.; Brown, E.; Rodenberg, N.; Jaeger, H.M.; Lipson, H. A positive pressure universal gripper based on the jamming of granular material. *IEEE Trans. Robot.* **2012**, *28*, 341–350. [CrossRef]
16. Najmuddin, A.; Fukuoka, Y.; Ochiai, S. Experimental development of stiffness adjustable foot sole for use by bipedal robots walking on uneven terrain. In Proceedings of the 2012 IEEE/SICE International Symposium on System Integration, Fukuoka, Japan, 16–18 December 2012; pp. 248–253.

17. Cheng, N.G.; Lobovsky, M.B.; Keating, S.J.; Setapen, A.M.; Gero, K.I.; Hosoi, A.E.; Iagnemma, K.D. Design and analysis of a robust, low-cost, highly articulated manipulator enabled by jamming of granular media. In Proceedings of the 2012 IEEE International Conference on Robotics and Automation, Guangzhou, China, 11–14 December 2012; pp. 4328–4333.
18. Hauser, S.; Eckert, P.; Tuleu, A.; Ijspeert, A. Friction and damping of a compliant foot based on granular jamming for legged robots. In Proceedings of the 2016 6th IEEE International Conference on Biomedical Robotics and Biomechatronics, Singapore, 26–29 June 2016; pp. 1160–1165.
19. Hauser, S.; Melo, K.; Mutlu, M.; Ijspeert, A. Fast state switching of a jamming-based foot. In Proceedings of the 8th International Symposium on Adaptive Motion of Animals and Machines (AMAM2017), Sapporo, Japan, 27–30 June 2017.
20. Hauser, S.; Mutlu, M.; Banzet, P.; Ijspeert, A.J. Compliant universal grippers as adaptive feet in legged robots. *Adv. Robot.* **2018**, *32*, 825–836. [CrossRef]
21. Tramsen, H.; Heepe, L.; Gorb, S.N. Granular Media Friction Pad—Soft vs. Stiff. *Appl. Sci.* **2021**, in press.
22. Drotlef, D.-M.; Stepien, L.; Kappl, M.; Barnes, W.J.P.; Butt, H.-J.; del Campo, A. Insights into the adhesive mechanisms of tree frogs using artificial mimics. *Adv. Funct. Mater.* **2013**, *23*, 1137–1146. [CrossRef]
23. Persson, B.N.J.; Tartaglino, U.; Albohr, O.; Tosatti, E. Rubber friction on wet and dry road surfaces: The sealing effect. *Phys. Rev. B* **2005**, *71*, 35428. [CrossRef]
24. Roberts, A.D. Squeeze films between rubber and glass. *J. Phys. D Appl. Phys.* **1971**, *4*, 423–432. [CrossRef]
25. Federle, W.; Barnes, W.J.P.; Baumgartner, W.; Drechsler, P.; Smith, J.M. Wet but not slippery: Boundary friction in tree frog adhesive toe pads. *J. R. Soc. Interface* **2006**, *3*, 689–697. [CrossRef]
26. Chen, H.; Zhang, L.; Zhang, D.; Zhang, P.; Han, Z. Bioinspired surface for surgical graspers based on the strong wet friction of tree frog toe pads. *ACS Appl. Mater. Interfaces* **2015**, *7*, 13987–13995. [CrossRef] [PubMed]
27. Varenberg, M.; Gorb, S.N. Hexagonal surface micropattern for dry and wet friction. *Adv. Mater.* **2009**, *21*, 483–486. [CrossRef]
28. Barnes, W.J.P.; Perez Goodwyn, P.J.; Nokhbatolfoghahai, M.; Gorb, S.N. Elastic modulus of tree frog adhesive toe pads. *J. Comp. Physiol. A* **2011**, *197*, 969–978. [CrossRef] [PubMed]
29. Gorb, S.N.; Scherge, M. Biological microtribology: Anisotropy in frictional forces of orthopteran attachment pads reflects the ultrastructure of a highly deformable material. *Proc. R. Soc. Lond. B* **2000**, *267*, 1239–1244. [CrossRef] [PubMed]
30. Büscher, T.H.; Buckley, T.R.; Grohmann, C.; Gorb, S.N.; Bradler, S. The evolution of tarsal adhesive microstructures in stick and leaf insects (Phasmatodea). *Front. Ecol. Evol.* **2018**, *6*, 69. [CrossRef]
31. Green, D.M.; Alberch, P. Interdigital webbing and skin morphology in the neotropical salamander genus *Bolitoglossa* (Amphibia; Plethodontidae). *J. Morphol.* **1981**, *170*, 273–282. [CrossRef] [PubMed]
32. Wei, H.; Wang, X. Biomimetic design of elastomer surface pattern for friction control under wet conditions. *Bioinspiration Biomim.* **2013**, *8*, 46001.
33. Barnes, W.J.P. Functional morphology and design constraints of smooth adhesive pads. *MRS Bull.* **2007**, *32*, 479–485. [CrossRef]
34. Kosaki, A.; Yamaoka, R. Chemical composition of footprints and cuticula lipids of three species of lady beetles. *Jpn. J. Appl. Entomol. Zool.* **1996**, *40*, 47–53. [CrossRef]
35. Rand, C.J.; Crosby, A.J. Friction of soft elastomeric wrinkled surfaces. *J. Appl. Phys.* **2009**, *106*, 64913. [CrossRef]
36. Barnes, W.J.P. Tree frogs and tire technology. *Tire Technol. Int.* **1999**, *99*, 42–47.
37. Barnes, W.J.P.; Smith, J.; Oines, C.; Mundl, R. Bionics and wet grip. *Tire Technol. Int.* **2002**, *2002*, 56–60.
38. Persson, B.N.J. Wet adhesion with application to tree frog adhesive toe pads and tires. *J. Phys. Condens. Matter* **2007**, *19*, 376110. [CrossRef]
39. Gorb, S.N.; Jiao, Y.; Scherge, M. Ultrastructural architecture and mechanical properties of attachmentpads in *Tettigonia viridissima* (Orthoptera Tettigoniidae). *J. Comp. Physiol. A* **2000**, *186*, 821–831. [CrossRef]
40. Federle, W.; Endlein, T. Locomotion and adhesion: Dynamic control of adhesive surface contact in ants. *Arthropod Struct. Dev.* **2004**, *33*, 67–75. [CrossRef] [PubMed]
41. Hanna, G.; Barnes, W.J.P. Adhesion and detachment of the toe pads of tree frogs. *J. Exp. Biol.* **1991**, *155*, 103–125. [CrossRef]
42. Federle, W.; Brainerd, E.L.; McMahon, T.A.; Hölldobler, B. Biomechanics of the movable pretarsal adhesive organ in ants and bees. *Proc. Natl. Acad. Sci. USA* **2001**, *98*, 6215–6220. [CrossRef]
43. Jiao, Y.; Gorb, S.N.; Scherge, M. Adhesion measured on the attachment pads of *Tettigonia viridissima* (Orthoptera, Insecta). *J. Exp. Biol.* **2000**, *203*, 1887–1895. [CrossRef] [PubMed]
44. Peressadko, A.G.; Hosoda, N.; Persson, B.N.J. Influence of surface roughness on adhesion between elastic bodies. *Phys. Rev. Lett.* **2005**, *95*, 124301. [CrossRef]
45. Heise, R.; Popov, V.L. Adhesive contribution to the coefficient of friction between rough surfaces. *Tribol. Lett.* **2010**, *39*, 247–250. [CrossRef]
46. Voigt, D.; Karguth, A.; Gorb, S.N. Shoe soles for the gripping robot: Searching for polymer-based materials maximising friction. *Robot. Auton. Syst.* **2012**, *60*, 1046–1055. [CrossRef]
47. Varenberg, M.; Gorb, S.N. Shearing of fibrillar adhesive microstructure: Friction and shear-related changes in pull-off force. *J. R. Soc. Interface* **2007**, *4*, 721–725. [CrossRef] [PubMed]

48. Varenberg, M.; Gorb, S.N. Close-up of mushroom-shaped fibrillar adhesive microstructure: Contact element behaviour. *J. R. Soc. Interface* **2007**, *5*, 785–789. [CrossRef]
49. Murarash, B.; Itovich, Y.; Varenberg, M. Tuning elastomer friction by hexagonal surface patterning. *Soft Matter* **2011**, *7*, 5553–5557. [CrossRef]